PROCEEDINGS, 48th Workshop on Geothermal Reservoir Engineering
Stanford University, Stanford, California, February 6-8, 2023
SGP-TR-224

Improved filtering for a new Resource Assessment Method

Andrew Power, Michael Gravatt, Ken Dekkers, Oliver Maclaren, Ruanui Nicholson, John O'Sullivan, Alex de Beer, Theo Renaud and Michael O'Sullivan

Department of Engineering Science, University of Auckland, Private Bag 92019, Auckland, New Zealand

jp.osullivan@auckland.ac.nz

Keywords: pre-exploration data, resource assessment uncertainty, geothermal potential energy, Waiwera

ABSTRACT

There remains a large economic risk in the exploration and development of a green field geothermal resource. Managing the economic risk of a green field project is done by assessing the potential of the new geothermal energy source. This is currently still done by stored heat calculations and applying an approximate recovery factor. The uncertainty of the parameters that go into a stored heat calculation can be quantified with Monty Carlo simulation however historically these estimates remain crude and often fail to accurately predict the potential of the resource. We have developed a new method for assessing the potential of a green field geothermal resource by using numerical modelling and uncertainty quantification. This new method uses the same available data as a stored heat calculation but also includes reservoir physics, wellbore physics, and realistic energy extraction scenarios. This method has shown interesting resource assessment results.

Currently, we have improved this method to include more data and information about the geothermal system in the pre-filtering of the steady-state sample models. This information includes, but is not limited to, the size and shape of the geothermal plume (distinctive for a geothermal system), the temperature outside the active reservoir, and surface features. Including more data on which to condition the steady-state samples improves the pre-filtering process. We have also shown the value of resampling. This method for resource assessment requires a large number of sample models that respect the natural state data. By generating sample models, filtering on the data, building a statistical model of the accepted samples and resampling, we significantly reduce the number of samples needed by increasing the number of samples that satisfy our acceptance criteria. Successive resampling may prove useful as an alternative to manual calibration when conditioning on reservoir engineering data.

1. INTRODUCTION

1.1 Geothermal Modelling

Numerical modelling is widely used in geothermal resource management as a tool to make predictions, including uncertainty quantification. These predictions are typically the temperature and pressure throughout the geothermal system which can then be used to assess the potential for a new geothermal field. Modelling can also provide information about the geology of a system, revealing details such as the permeabilities of various rock types or the strengths of deep upflows; however, these are often not of direct interest. Indeed, this paper focuses on a novel approach of reducing the uncertainty in temperature predictions with the belief that this could lead to more certain estimates of power output.

1.2 Motivation

Currently, the most common method of estimating the power output of a geothermal field is through a stored heat calculation (Zarrouk & Simiyu, 2013; Ciriaco, Zarrouk, & Zakeri, 2019). Monte Carlo simulation is typically used to quantify the uncertainty in any predictions (Athens & Caers, 2019; Dekkers, et al., 2022) but this does not make use of any geophysics known about the field. A roughly estimated recovery factor is then applied which further adds uncertainty to the estimate. In oil & gas (and geothermal) technical specialists estimate ranges between the 10th and 90th percentiles values for geological parameters. These ranges have been shown to contain the true value (once it becomes known) less than 50% of the time, rather than the expected 80% (Hawkins et al., 2002). This issue is amplified in the case of a green field resource where the system is largely unexplored, and less data exists. Growing climate concerns are fuelling a desire for more renewable energy sources, and geothermal energy remains under-utilised around the world. The exploration of geothermal green fields offers the perfect opportunity to harness some of the untapped potential of geothermal energy while also providing a pathway to a cleaner energy future. However, unexplored geothermal fields pose significant economic risks as a failed well can often cost several millions of dollars (Beckers, et al., 2013).

1.3 A New Approach

To mitigate these risks, a new method for resource estimation is proposed which makes use of additional data in a novel way. Although this data has been available for a long time and may appear obvious to an expert, it has never been incorporated into resource estimation and uncertainty quantification. The use of additional data in this new approach could enable the estimation of the resource potential with greater accuracy and less uncertainty. The benefits of this approach include a better ability to manage the resource effectively in the long term, and a better understanding of the economic viability of a green field resource thus encouraging for greater investment into the sector.

The method developed involves simulation-based inference followed by geophysical informed feature extraction by applying a series of filters to the simulated steady-state models corresponding to the natural state of the geothermal reservoir. Parallel execution, geothermal flow simulators like Waiwera (Croucher, O'Sullivan, O'Sullivan, Yeh, & Burnell, 2020) developed at the University of Auckland's Geothermal Institute allow such a large number of model realisations to be a feasible approach. Having a large number of prior samples can also systematically incorporate uncertainty into any predictions. The result of applying these filters is an objective function value for each sample model, and the ability to rank the sample models according to how well they fit each condition. The best steady-state sample models could then be run through a maximum production potential scenario to estimate the power output of the geothermal field using a method outlined by Dekkers et al. (2022). Further, the underlying model parameters, such as the rock type permeabilities and deep mass upflows, of the best sample models can be used to fit a joint Gaussian distribution from which new, physically informed geothermal models can be generated through resampling.

This paper will discuss the methodology used to select the most geophysically informed models, as well as an evaluation of the effectiveness of resampling as a means of generating new models that obey simple geological principles.

2. METHODOLOGY

2.1 The Numerical Model

The computational model used throughout this paper is a synthetic three-dimensional model developed to be representative of a typical New Zealand geothermal system. It comprises 11,764 blocks of varying sizes with greater definition towards the centre of the grid and spans an area of 13km by 15km with a maximum depth of -3,250m below sea level. There are three faults, each defined by their own rock types, and an alteration zone identified by a clay cap as shown in Figure 1 (Renaud, et al., 2021).

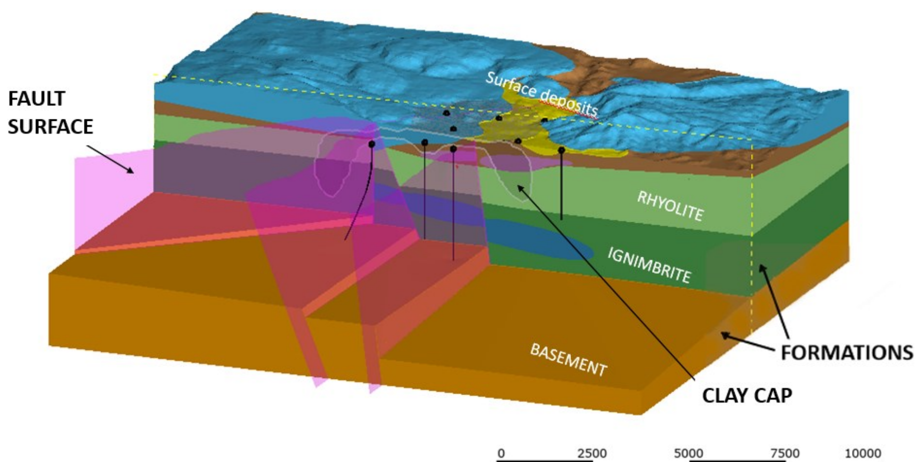

Figure 1: Conceptual model of the synthetic geothermal model (Renaud, et al., 2021).

<u>2.1.1 Uncertain Model Parameters</u>

The parameters of interest are the rock type permeabilities, and the deep mass upflows. There are 82 different rock types each with an associated x-, y-, and z-permeability, as well as 24 potential mass flow rates giving a total of 270 model parameters. These 24 mass flow rates correspond to the 24 blocks on the base of the computational model that lie on at least one fault; no other blocks were considered as a source of fluid flow.

The prior parameter values for each sample are assigned using a novel approach outlined in an accompanying paper by de Beer et al. (2023). This approach makes use of geological principles to ensure that the parameters are consistent with what is observed in reality. Each rock formation is assigned a base rock type with an associated set of log-normally distributed permeabilities. These are multiplied by a set of modifiers to produce the permeabilities of the rock types within the formation that are found in the clay cap, on a fault, and at the intersections of multiple faults. There is also correlation enforced between the x-, y-, and z-permeabilities for each base rock type with the x- and y-permeabilities having a correlation coefficient of 0.8, and the z-permeabilities having a correlations coefficient of 0.5 with both the x- and y-permeabilities.

All of the modifiers were sampled from log-normal distributions; however, these distributions were constrained to impose geological realism on the sample models. For the blocks in the low conductivity alteration zone, the permeabilities cannot be more than those of the base rock types and so the modifiers were restricted to be less than or equal to one. The modifiers corresponding to the permeabilities along or up a fault were constrained to be greater than or equal to one so that these blocks allow fluid to flow more easily than the base rock type. Finally, the modifiers of the permeabilities across a fault were restricted to be less than or equal to one to reflect the fact that it is more difficult for fluid to flow across a fault.

The 24 deep upflows are also random and drawn from a multivariate Gaussian distribution with a correlation imposed so that blocks along a fault in close proximity have similar mass flow rates. Subsequently, these upflows in each sample model are scaled so that the distribution of total mass flow rates over all of the sample models is uniformly distributed between 30 and 70kg/s. The details of both of these processes are described in de Beer et al. (2023).

2.2 Running the Model

Simulation-based approaches generally require a large number of sample models to be generated especially when attempting to quantify the uncertainty associated with the results. In this paper 2,000 models were generated and run through to steady state with 1,785 (89.2%) of these sample models converging. Therefore, for this approach to be feasible it is highly dependent on the computational efficiency of the simulator. Waiwera is a geothermal flow simulator developed by the University of Auckland's Geothermal Institute and GNS Science (Croucher, O'Sullivan, O'Sullivan, Yeh, & Burnell, 2020) that is capable of parallel execution which allows for multiple models to be run at the same time greatly increasing efficiency. Therefore, the large number of simulations can be handled and uncertainty quantification can be carried out reliably and accurately.

2.3 The Filters

This paper considers two criteria by which the sample models can be ranked. Both involve an objective function that measures how well a sample model conforms to the expected behaviour and it is this objective function value that is used to rank the sample models. In both cases, sample models with a lower objective function value are said to have performed better. The details of these two filters are discussed below.

2.3.1 Temperature Outside the Geothermal Reservoir

The first pre-processing filter applied to the steady-state sample models is one to ensure that the temperatures outside the reservoir are as cool as would be expected in the Earth's crust if a geothermal system were not present. This region outside the reservoir is defined to be any blocks in the computational model that are not underneath the clay cap. By imposing an upper bound on the temperatures in certain blocks in the model, we restrict the size of the geothermal plume and prevent hot fluid leaking out of the reservoir, thus leading to more realistic systems. This process requires no additional data other than an awareness of where the clay cap is located in the system, and the temperature gradient in the Earth's crust. This research assumes a constant temperature gradient of 30°C/km (Fridleifsson, et al., 2008; Earle, 2019), although this value varies locally.

First, predicted temperatures are calculated for every block in the model outside of the geothermal reservoir. This is done by taking the temperature of the surface block in each column as the true temperature, and then using the 30°C/km temperature gradient to calculate a predicted temperature in each block dependent on the depth below the surface block. A multiplicative safety factor of 1.5 is applied to these predicted temperatures to account for any potential inaccuracies in estimating the temperature gradient in the Earth's crust or the effects of random noise in the model results. Then, the differences between the model temperatures and the predicted temperatures for each sample are calculated. Since the objective of this filter is to ensure that the area outside the reservoir is no hotter than it should be, in any block where the model temperature is less than the predicted temperature, the difference is taken to be zero so that cooler systems are not penalised. Finally, the sum of squared differences for each sample model is calculated to give an overall measure of how near the sample models are to that of a typical geothermal system, i.e.,

$$S_i = \sum_{j=1}^{N_{outside}} \left(\max\left\{0, T_{i,j}^{(M)} - s \times T_{i,j}^{(P)}\right\}\right)^2$$

where, S_i is the score for each sample i, $T_{i,j}^{(M)}$ is the model temperature for block j in sample model i, s is the safety factor, $T_{i,j}^{(P)}$ is the predicted temperature for block j in sample model i, and $N_{outside}$ is the number of blocks outside the geothermal reservoir.

2.3.2 Temperature beneath the Clay Cap

The second filter that is applied to the sample models is based on the temperature required for the clay cap of a geothermal system to form. This typically occurs when the temperature of the fluid reaches 180-200°C (Maza, et al., 2018; Gunderson, Cumming, Astra, & Harvey, 2000). Assuming the location of the clay cap is known, the block directly below the clay cap in each column of the computational model must have been at approximately this temperature at some point in its history for the clay cap to form. Since we are focusing on steady-state models, we can say that the temperature just beneath the clay cap should still be approximately 190°C and this was the temperature used in the calculations.

As the location of the clay cap is often not precisely known, especially in a geothermal green field, not all of the blocks in the model just beneath the clay cap were considered in this calculation. The deepest of these, which are typically those on the edge of the clay cap, were disregarded as they had the largest variations in temperature and a disproportionate effect on the objective function compared to the blocks closer to the centre of the clay cap. Thus 60% of the blocks just beneath the clay cap were used in the calculations as shown in Figure 2.

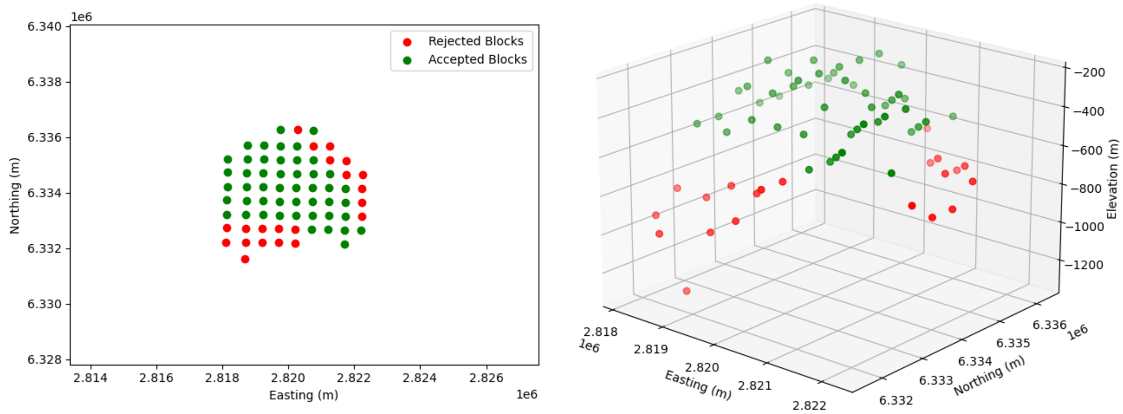

Figure 2: A 2D, top-down view (left) and a 3D view (right) of which blocks were included (green) and disregarded (red).

First, the absolute differences between the model temperatures and the temperature required for the formation of the clay cap were calculated. By taking the absolute value of the differences, systems that were either too hot or too cold were penalised equally as there is a distinct temperature to which the models should be close. Next, the sum of absolute differences for each sample is calculated to give a measure of how geologically reasonable each sample is, i.e.,

$$S_i = \sum_{j=1}^{N_{claycap}} \left\| T_{i,j}^{(M)} - T^{(CC)} \right\|$$

where, S_i is the score for each sample model i, $T_{i,j}^{(M)}$ is the model temperature for block j in sample model i, $T^{(CC)}$ is the expected temperature just beneath the clay cap, and $N_{claycap}$ is the number of blocks just beneath the clay cap used in the calculations.

2.4 Resampling Model Parameters from a Joint Gaussian Distribution

As the computational models can require a significant amount of time to run especially for a large number of models, being able to generate additional sample models that are geologically reasonable is beneficial. To achieve this, the model parameter values that give rise to the accepted sample models after filtering can be used to fit a multivariate Gaussian distribution from which further parameter sets can be resampled.

Sampling from the joint Gaussian distribution requires the mean vector $\boldsymbol{\mu}$ and covariance matrix C of the $k = 1, 2, \ldots, K$ random variables, or model parameters, based on the $i = 1, 2, \ldots, N$ accepted sample models. Let $\boldsymbol{X}$ be the random vector whose kth element is one of the random variables. The sample mean is given by

$$\mu_k = \frac{1}{N}\sum_{i=1}^{N} \boldsymbol{X}_{ik}$$

where μ_k is the sample mean of the kth model parameter. Similarly, the covariance matrix can be computed as

$$C_{jk} = \frac{1}{N-1}\sum_{i=1}^{N}(\boldsymbol{X}_{ij} - \mu_j)(\boldsymbol{X}_{ik} - \mu_k)$$

where C_{jk} is the covariance between the jth and kth model parameters (Johnson & Wichern, 2007).

Generating a new sample model from the multivariate Gaussian distribution then requires sampling from the standard normal distribution, i.e., $r \sim \mathcal{N}(\boldsymbol{0}, I)$, and performing a Cholesky decomposition on the covariance matrix such that $C = LL^{\mathrm{T}}$. A sample can be simulated by calculating

$$\boldsymbol{\theta}_s = \boldsymbol{\mu} + Lr$$

where $\boldsymbol{\theta}_s$ is the simulated sample of model parameters, $\boldsymbol{\mu}$ is the mean vector of the parameters, L is the Cholesky decomposition of the covariance matrix, and r is a realisation from the standard normal distribution (Orduz, 2019). The process of fitting a joint Gaussian distribution and sampling from it is carried out using the *ccandu* Python package (Modelling Uncertainty and Data Group UoA, 2021).

3. RESULTS

3.1 The Effects of Filtering

3.1.1 Temperature Outside the Geothermal Reservoir

After the first filter is applied to the 1,785 prior samples, objective function values and subsequent rankings are used to select the 350 best sample models based on how close they are to the predicted temperature outside the geothermal reservoir. These 350 best sample models form the posterior distribution, the characteristics of which can be compared to those of the prior ensemble. Figure 3 shows an accepted sample model and a rejected sample model according to this condition. It is evident that worse sample models are hotter over a greater area, with temperatures close to 300°C, and tend to be larger geothermal systems with hot fluid leaking further than expected. Conversely, better sample models have hot fluid concentrated over a smaller area with little leakage, although the temperature can still reach close to 300°C.

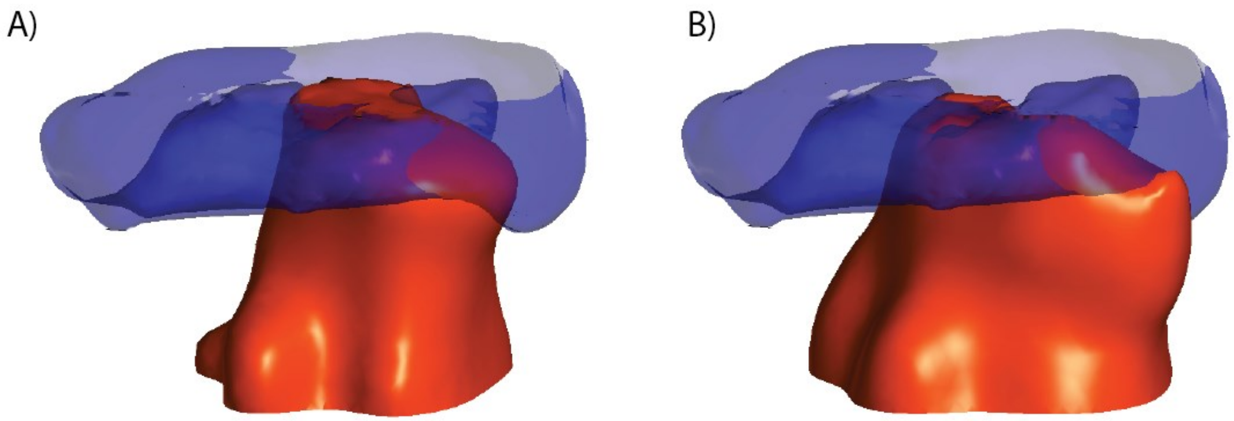

Figure 3: The geothermal plumes of an accepted sample (A) and a rejected sample (B) after filtering based on the temperature outside the geothermal reservoir. The clay cap is also shown for context and the 190°C isotherm is shown in orange.

The posterior distributions also show differing characteristics when viewed in the parameter space. The distribution of total mass flows, as can be seen in Figure 4, suggests that models with lower total mass flow rates are favoured. Inspection of the individual mass flows also reveals that, in each of the blocks where mass flow was considered, the accepted sample models have lower flow rates on average than the prior samples. It also appears that, in most cases, higher permeabilities are found in the accepted sample models and with greater certainty which is evident in the shifted means and lower variances of the marginal densities of the rock type shown in Figure 4. These changes are more prominent in the z-permeabilities than the x- or y-permeabilities. The upper scatter plots in Figure 4 show the confidence ellipses of the accepted sample models (black) overlaid on those of the prior samples (grey) with the distance between each ellipse representing one standard deviation from the mean. From this, it can be seen that the correlations with the z-permeability strengthen as a result of the filtering process as does, to a lesser extent, the correlation between the x- and y-permeabilities.

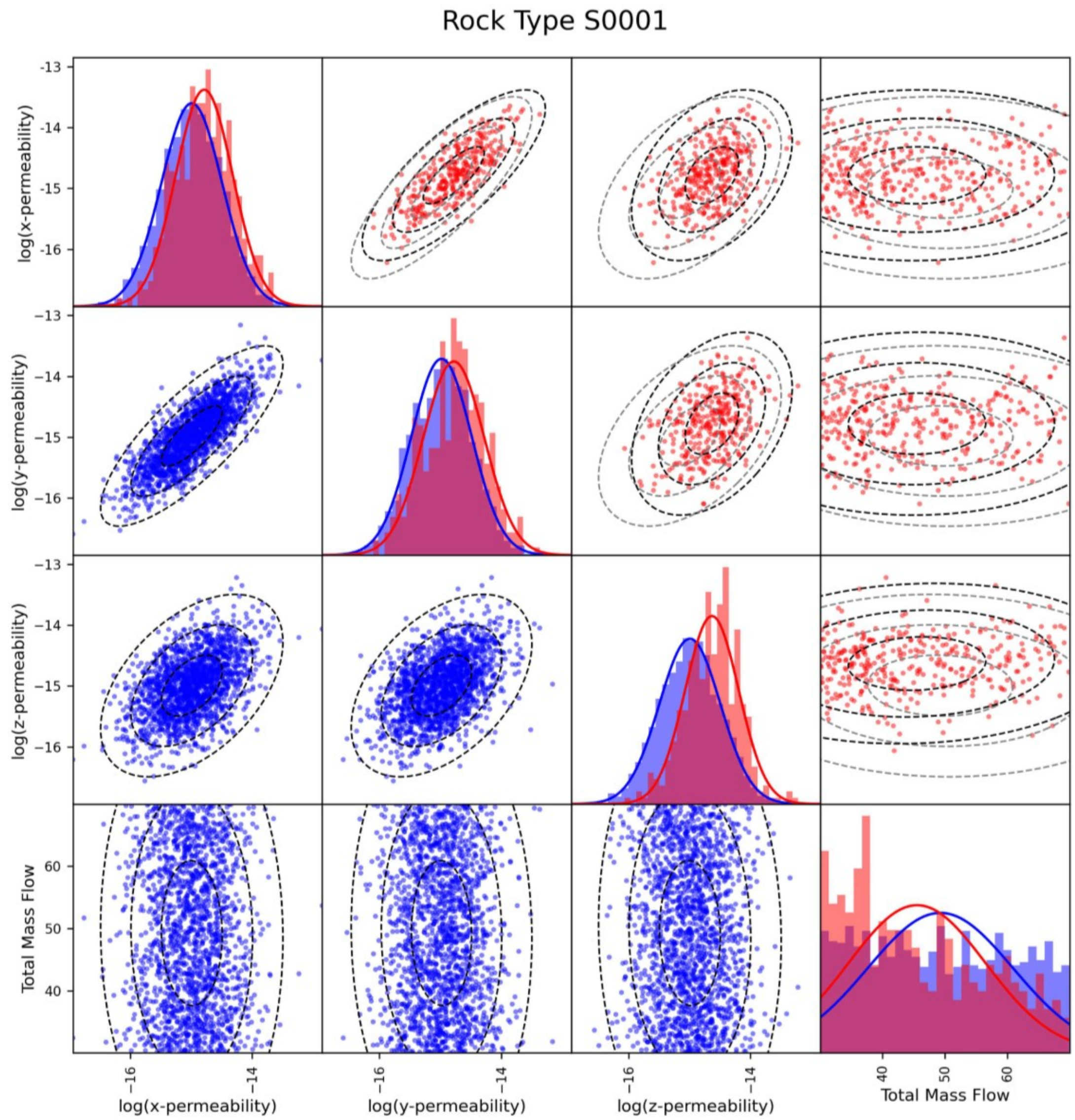

Figure 4: Correlations and marginal densities for the x-, y-, and z-permeabilities of a representative rock type before (blue) and after (red) conditioning on the temperature outside the geothermal reservoir.

3.1.2 Temperature Beneath the Clay Cap

In a similar way to the previous filter, objective function values and rankings are used to select the 350 best sample models from the prior ensemble based on how close the temperature beneath the clay cap is to 190°C. An accepted sample model and a rejected sample model according to this condition can be seen in Figure 5. Conversely to the previous filter, worse sample models tend to be smaller, colder geothermal systems where there is not enough heat in the system to adequately meet the expected temperature. Warmer, deeper systems also rank lower as the heat fails to reach the elevation of the clay cap. There are systems that perform poorly due to being too hot, but this behaviour is infrequent compared to the cooler systems. Better sample models appear to be larger and hotter in nature, although some comprise narrow geothermal plumes that expand near the elevation of the clay cap.

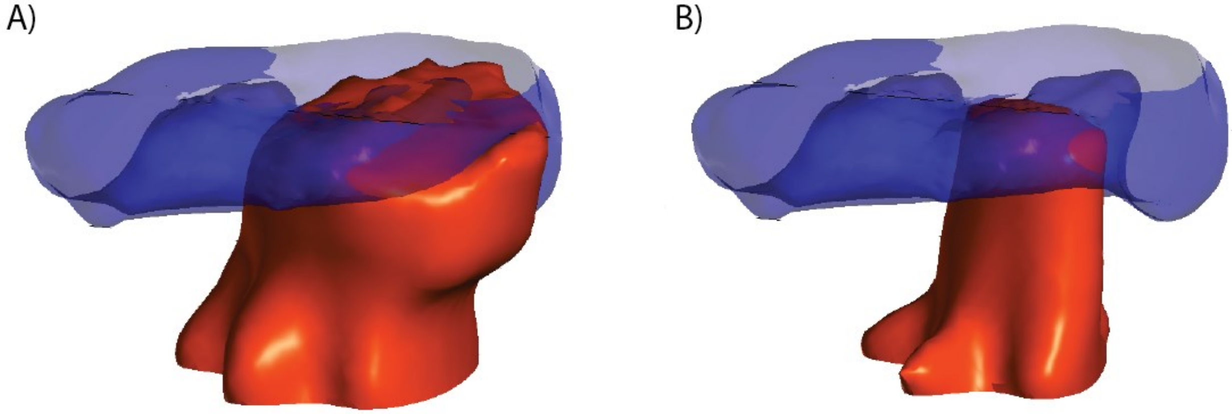

Figure 5: The geothermal plumes of an accepted sample model (A) and a rejected sample model (B) after filtering based on the temperature just beneath the clay cap. The clay cap is also shown for context and the 190°C isotherm is shown in orange.

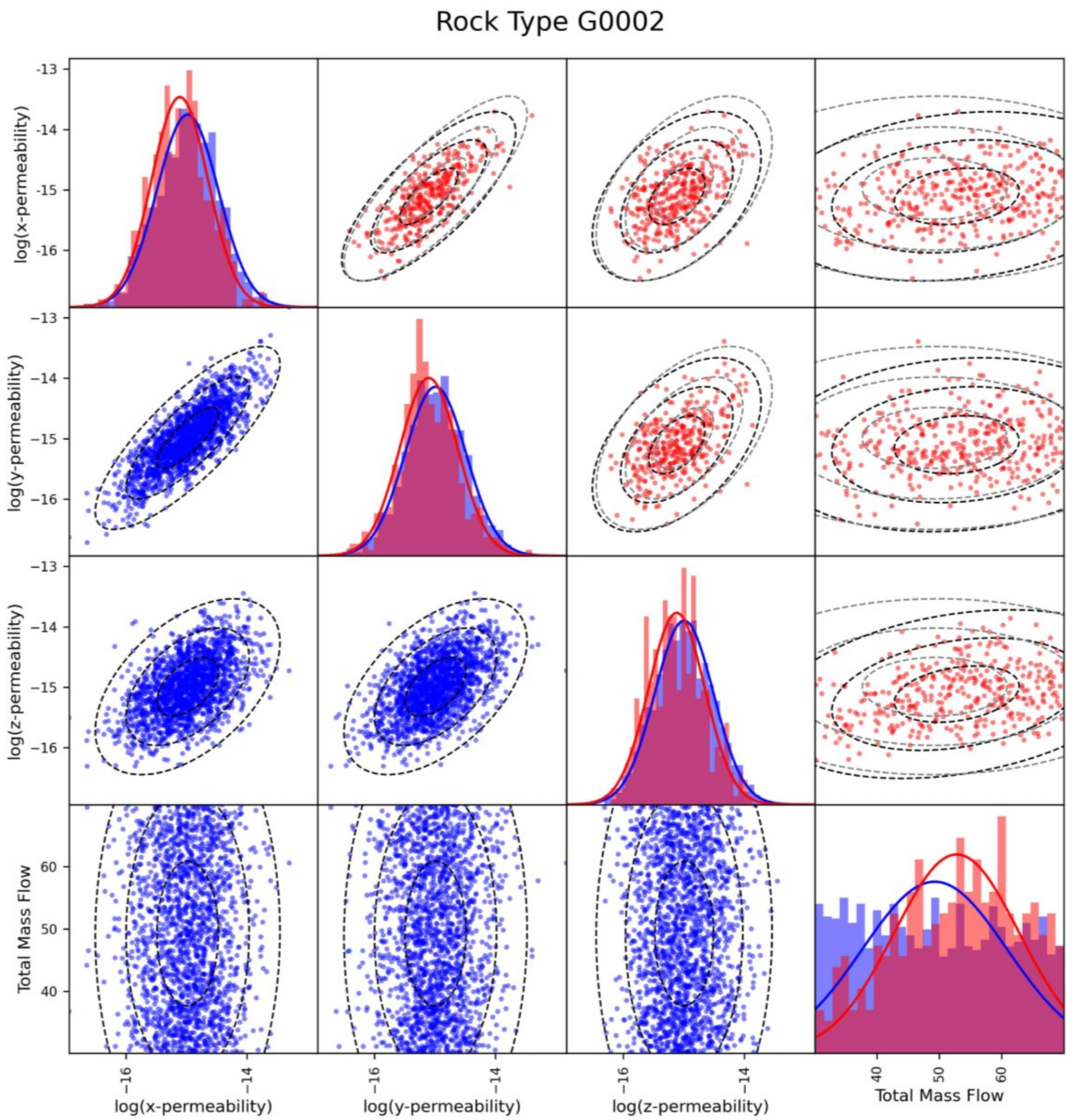

Figure 6: Correlations and marginal densities for the x-, y-, and z-permeabilities of a representative rock type before (blue) and after (red) conditioning on the temperature just beneath the clay cap.

Again, the accepted sample models show different characteristics to the prior samples in the parameter space as well and the data space. Filtering the sample models based on the temperature beneath the clay cap heavily favours models with higher mass flow rates as can be seen by the posterior total mass flow distribution in Figure 6 shifting towards larger flow rates. The same is also true in all of the individual mass flows. There is a less discernable effect on the permeabilities of the rock types, however, in the majority of rock types, smaller permeability values tend to be preferred as can be seem to a small extent in Figure 6. This filter also seems to introduce some correlation between the rock type permeabilities and the total mass flow which is not apparent when using the previous filter. The confidence ellipses in the posterior scatter plots between the permeabilities and total mass flow in Figure 6 show a shift from no correlation to a slight positive correlation. This is most distinguishable when looking at the relationship between the z-permeability and the total mass flow.

3.1.3 Using Both Filters Consecutively

To find sample models that respect both geological principles being considered, both of the filters are applied to the prior sample models consecutively. First, the filter based on the temperature outside the geothermal reservoir is applied to all 1,785 prior sample models and the best 700 sample models according to this condition are retained. The filter based on the temperature just beneath the clay cap is then applied to the remaining 700 sample models with the 350 best sample models being accepted and forming the posterior ensemble. This has the effect of removing a large number of the extreme geothermal systems that are either too large and hot or too small and cold leaving well-balanced systems that meet both conditions reasonably well. As such, better performing sample models seem to have a hot geothermal plume constrained mainly to be beneath the clay cap without leaking hot fluid into the rest of the system.

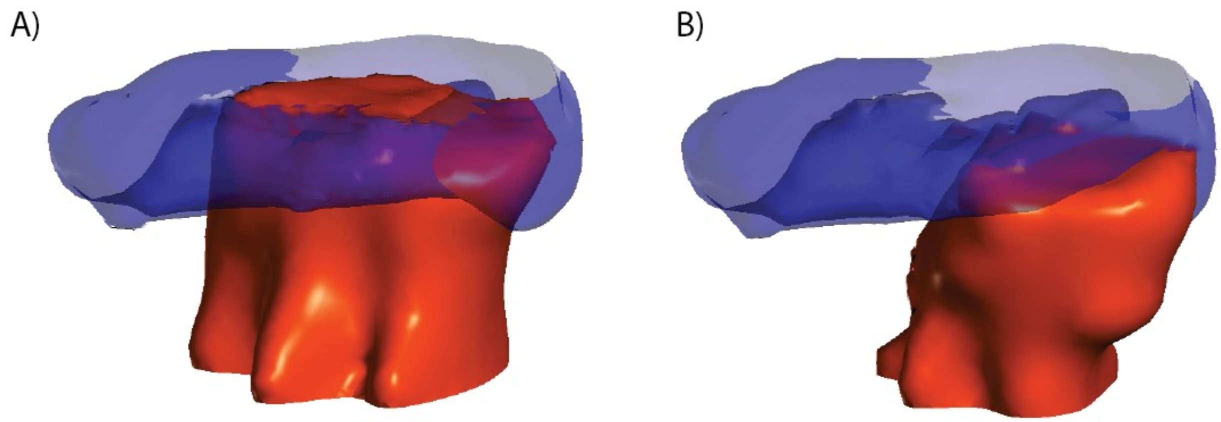

Figure 7: The geothermal plumes of an accepted sample model (A) and a rejected sample model (B) after filtering first based on the temperature outside the geothermal reservoir and then on the temperature just beneath the clay cap. The clay cap is also shown for context and the 190°C isotherm is shown in orange.

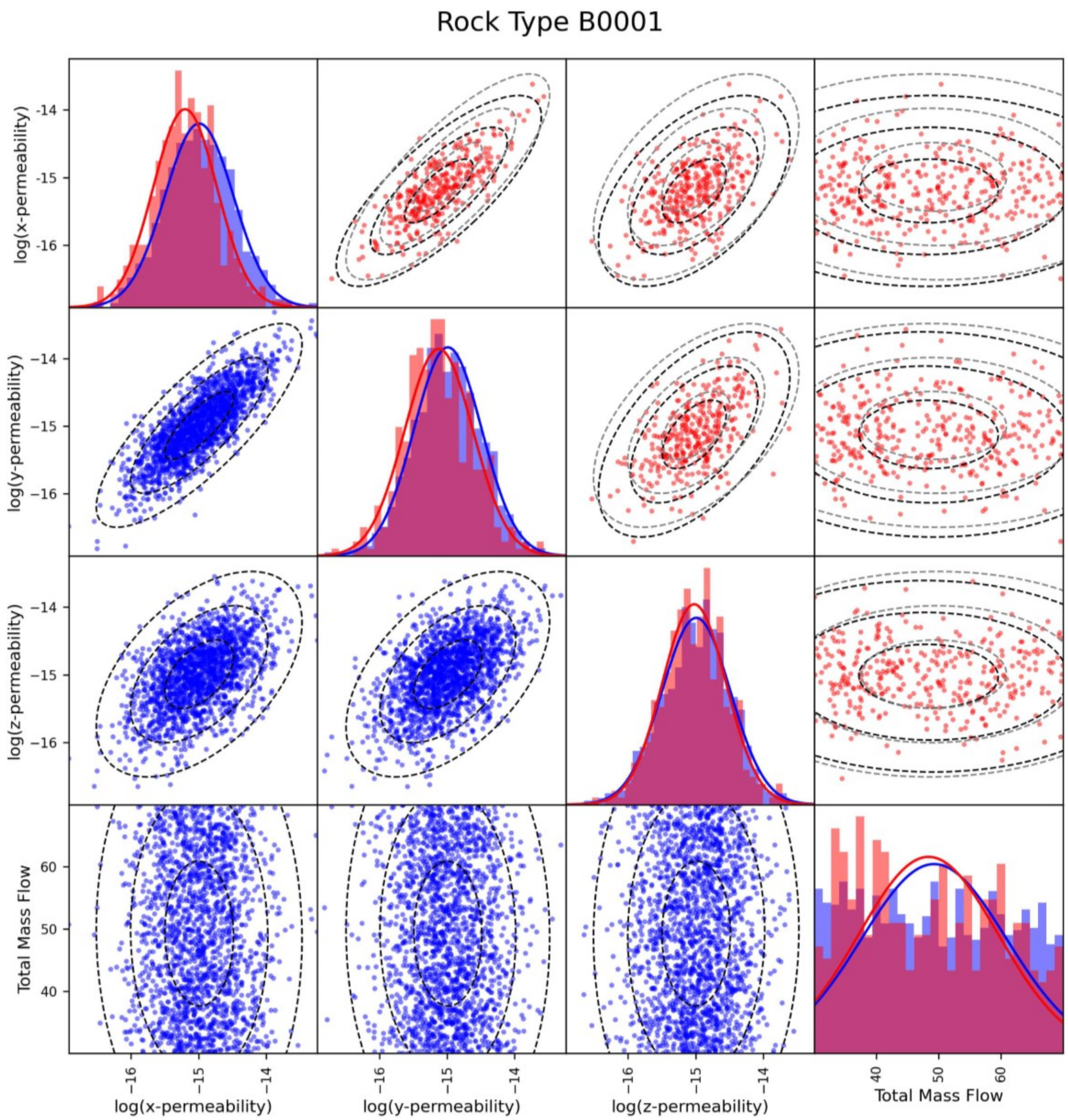

Figure 8: Correlations and marginal densities for the x-, y-, and z-permeabilities of a representative rock type before (blue) and after (red) conditioning on both the temperature outside the geothermal reservoir and the temperature just beneath the clay cap.

While the merit of this combined filtering approach is apparent when looking in the data space, the effects are less well-defined in the parameter space. The distribution of total mass flows does not change significantly between the prior and posterior sample models as shown in Figure 8. The mass flow rates of individual blocks also have mixed results with some preferring smaller and some preferring larger mass flow rates. While there is no overall trend in the direction of preference of rock permeabilities, rock types within the same rock formation appear to share characteristics, and the rock formations behave differently. B (FULL NAME) rock types favour smaller rock permeabilities as can be seen in Figure 8, D and S rock types favour larger rock permeabilities, and other rock types show either no preference or small shifts in both directions.

3.2 The Effects of Resampling Parameter Values

After the filters have been applied in each of the three scenarios detailed above, multivariate Gaussian distributions are fitted to the model parameters of the accepted sample models. In each case, the best 350 prior sample models are used to fit the distribution and 1,000 realisations are sampled from the resulting joint Gaussian distribution and run through to steady state. To see whether this resampling process generates a higher proportion of geologically reasonable models, the same filtering process that was applied to the prior sample models is also applied to the resampled models. The results for each of the three scenarios is now discussed.

The filter based on the temperature outside the geothermal reservoir was applied to the 1,785 prior sample models and a joint Gaussian distribution was fitted using the model parameters of the 350 best sample models. Of the 1,000 resampled models, 880 converged when run through to steady state giving a convergence rate of 88.0% which is slightly less than that of the prior sample models where 89.2%

converged. Further, 699 of the 880 resampled models (79.4%) had an objective function value less than the threshold at which the prior sample models were accepted. This indicates that the new sample models are more than four times as likely to satisfy the geological principle on which the filter is based.

Figure 9 shows the objective function of the prior sample models in black and the objective function value threshold at which the best sample models are determined in blue. Similarly, the objective function corresponding to the resampled models is shown in red, and it can be seen that the proportion of sample models satisfying the acceptance threshold increases from 19.6% to 79.4%.

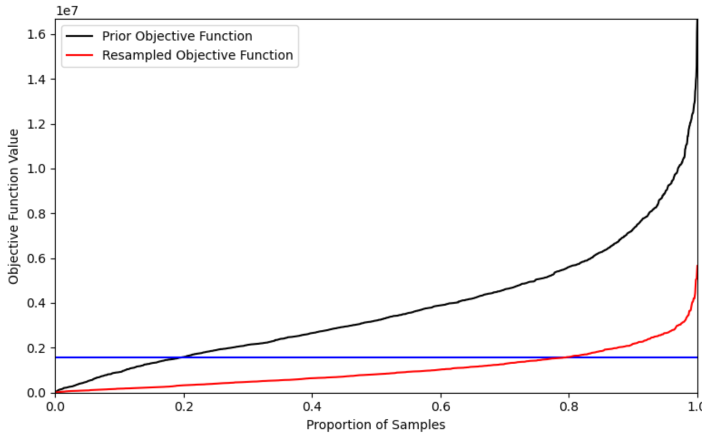

Figure 9: Objective functions of the prior (black) and resampled (red) models when they are filtered based on the temperature outside the geothermal reservoir.

The filter based on the temperature underneath the clay cap was also applied to the 1,785 prior sample models and a new joint Gaussian distribution was fitted using the model parameters of the 350 best sample models. Of the 1,000 resampled models, 898 converged when run through to steady state giving a convergence rate of 89.8% which is slightly more than that of the prior sample models. Compared to the previous filter, a smaller proportion of the resampled models had an objective function value less than the threshold at which the prior sample models were accepted with 601 of the 898 sample models (66.9%). However, this still suggests that the resampled models are more than three times as likely to have an appropriate temperature just beneath the clay cap than the prior sample models. These results are shown in Figure 10.

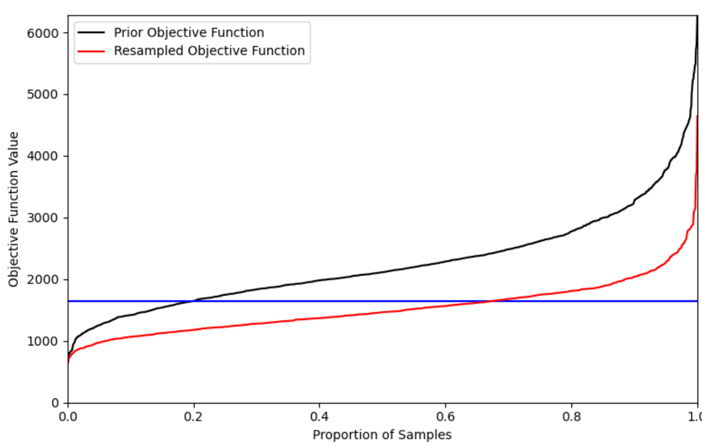

Figure 10: Objective functions of the prior (black) and resampled (red) models when they are filtered based on the temperature beneath the clay cap.

Finally, both of the two filters were applied consecutively to the 1,785 prior sample models and another joint Gaussian distribution was fitted using the model parameters of the 350 best sample models. Of the 1,000 resampled models, 894 converged when run through to steady state giving a convergence rate of 89.4% which is slightly more than that of the prior sample models. The filter based on the temperature outside the geothermal reservoir was applied to the 894 resampled models and any sample models that had an objective function value better than the acceptance threshold from the prior sample models were retained. This led to 715 of the 894 resampled models (80.0%) being accepted by the first filter which is more than twice that of the prior sample models where 700 of the 1,785 sample models (39.2%) were accepted. The filter based on the temperature underneath the clay cap was then applied to the remaining 715 resampled models, of which 542 (75.8%) had an objective function value better than that of the acceptance threshold from the prior sample models. Overall, 542 of the 894 resampled models (60.6%) satisfy both of the conditions compared to 350 of the 1,785 prior sample models (19.6%) showing that three times as many of the resampled models gave rise to geologically reasonable models. The objective functions and acceptance proportions of applying both filters to the prior and resampled models can be seen in Figure 11.

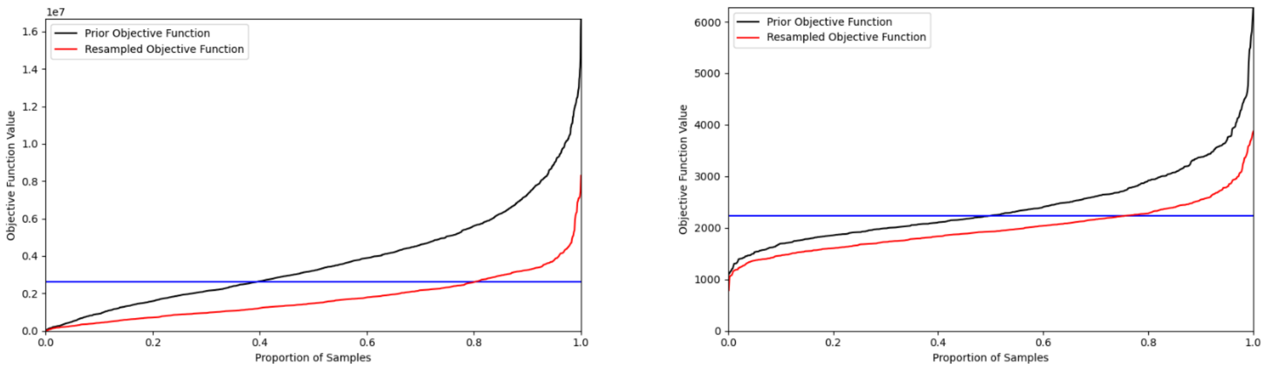

Figure 11: Proportions of simulations below the acceptance threshold when they are filtered first based on the temperature outside the geothermal reservoir (left) and then based on the temperature beneath the clay cap (right).

4. CONCLUSIONS

This paper has considered the feasibility and potential benefits of filtering steady-state models corresponding to the natural state of the geothermal reservoir. The filters were based on geological principles that are true of most geothermal systems and serve the purpose of refining the sample models used in a simulation-based approach from representing broad, naïve prior beliefs to being more geophysically informed. These geothermal consistent sample models should reduce the uncertainty in any temperature or pressure predictions, which can then be propagated forward to give power output estimates with less uncertainty and risk. This is paramount in geothermal green fields where information is scarce and the financial risks are significant.

The two filters used promote opposing characteristics in a geothermal system which reduces any redundancy. Conditioning the sample models on the temperature outside the geothermal reservoir favours smaller, cooler systems which are less likely to leak hot geothermal fluid into the surrounding rock. Conditioning on the temperature beneath the clay cap has the opposite effect, preferring larger, hotter systems that were more likely to contain hot geothermal fluid at the elevation of the clay cap. Combining these two filters resulted in more balanced geothermal systems being accepted with few extremes and characteristics of both filters present. These accepted sample models tended to feature a contained, hot geothermal plume directly underneath the clay cap which satisfies both of the conditions and adequately reflects geothermal systems that exist in reality. This suggests that the filtering approach can be used to effectively to remove unreasonable geothermal systems before they are run through maximum production potential scenarios which saves computational time and resources and allows resource estimates to be made with less uncertainty. While these filters are fairly simplified, it is possible to add complexity to the objective functions on which the filters are based with the addition of expert knowledge about the system.

The effect of filtering was also noticeable in the parameter space of the model which allowed for new, geologically consistent models to be generated by resampling from a multivariate Gaussian distribution fitted to the model parameters of the accepted sample models. This resampling approach resulted in at least three times as many of the resampled models being accepted by the filtering process than the prior models. Resampling did not lead to a significant improvement in the convergence rate of the simulations, but, as the model used for this research is very robust, improvements may be seen in more complex models with greater sensitivity on the model parameters.

This work sits in a broader area of research. By using numerical modelling and simulation based inference methods, we have developed a new method for assessing the resource potential of a green field geothermal resource. This filtering approach allows predictions of the temperature in the system which incorporate more data than previously. This is beneficial for estimating the resource potential and power output of a geothermal green field where data is sparse. The aim is to minimize financial risk so investors can make more robust decisions.

5. FUTURE WORK

Filtering models on additional data should be the next step in this pre-processing approach to simulation-based inference. Being able to refine the geothermal systems produced should lead to more accurate estimates made with more certainty. However, the filters need to be carefully constructed so as to not unnecessarily limit the scope of the geothermal systems by disregarding plausible models. Additional data could include conditioning on the temperatures of surface features in the geology of the model or conditioning on pressure data rather than focusing entirely on temperature data. A variation on the consecutive application of both filters could be explored where a combined objective function is designed to incorporate features of all geological principles resulting in only one filtering step being required rather than two.

There is also the potential to carry out the resampling process more than once. Investigating the effectiveness of filtering and fitting a multivariate Gaussian to the best of the resampled models could be useful in being able to generate even more geophysically reasonable geothermal systems. However, it is likely that filtering and resampling multiple times will have diminishing returns.

The underlying statistical distribution for the majority of this research has been based on a Gaussian distribution. While this encodes information about the prior beliefs well, there is no reason not to use other probability distributions during the sampling processes. Future work could assess the suitability of other methods for modelling the distributions of rock type permeabilities and deep mass upflows.

Finally, it would be beneficial to carry out this research on a more complex, real-world geothermal model. While the synthetic model used in this paper is representative of real geothermal systems, it is also well behaved which could lead to better than normal results.

REFERENCES

Athens, N. D., & Caers, J. K. (2019). A Monte Carlo-based framework for assessing the value of information and development risk in geothermal exploration. *Applied Energy*.

Beckers, K. F., Lukawski, M. Z., Reber, T. J., Anderson, B. J., Moore, M. C., & Tester, J. W. (2013). Introducing Geophires V1.0: Software package for estimating levelized cost of electricity and/or heat from enhanced geothermal systems. *Proceedings, 38th Workshop on Geothermal Reservoir Engineerings.* Stanford, California.

Ciriaco, A. E., Zarrouk, S. J., & Zakeri, G. (2019). Geothermal resource and reserve assessment methodology: Overview, analysis and future directions. *Renewable and Sustainable Energy Reviews*.

Croucher, A., O'Sullivan, M., O'Sullivan, J., Yeh, A., & Burnell, J. (2020). Waiwera: A parallel open-source geothermal flow simulator. *Computers and Geosciences*.

de Beer, A., Gravatt, M. J., Nicholson, M. O., Dekkers, K., O'Sullivan, J. P., Power, A., . . . O'Sullivan, M. J. (2023). Geologically Consistent Prior Parameter Distributions for Uncertainty Quantification of Geothermal Reservoirs. *Proceedings, 48th Workshop on Geothermal Reservoir Engineering.* Stanford, California.

Dekkers, K., Gravatt, M., Maclaren, O. J., Nicholson, R., Nugraha, R., O'Sullivan, M., . . . O'Sullivan, J. (2022). Resource Assessment: Estimating the Potential of a Geothermal Reservoir. *Proceedings, 47th Workshop on Geothermal Reservoir Engineering.* Stanford, California.

Earle, S. (2019). *Physical Geology - 2nd Edition.* Victoria, B.C.: BCcampus.

Fridleifsson, I. B., Bertani, R., Huenges, E., Lund, J. W., Ragnarsson, A., & Rybach, L. (2008). The possible role and contribution of geothermal energy to the mitigation of climate change. *IPCC Scoping Meeting on Renewable Energy Sources, Proceedings*, 59-80.

Gunderson, R., Cumming, W., Astra, D., & Harvey, C. (2000). Analysis of smectite clays in geothermal drill cuttings by the methylene blue method: for well site geothermometry and resistivity sounding correlation. *Proceedings World Geothermal Congress*, (pp. 1175-1181). Kyushu - Tohoku, Japan.

Hawkins, J. T., Coopersmith, E. M., and P. C. Cunningham. (2002): Improving Stochastic Evaluations Using Objective Data Analysis and Expert Interviewing Techniques. Paper presented at the SPE Annual Technical Conference and Exhibition, San Antonio, Texas, September 2002.

Johnson, R. A., & Wichern, D. W. (2007). *Applied Multivariate Statistical Analysis.* Hoboken, New Jersey: Pearson Prentice Hall.

Maza, S. N., Collo, G., Morata, D., Lizana, C., Camus, E., Taussi, M., . . . Rivera, G. (2018). Clay mineral associations in the clay cap from the Cerro Pabellón blind geothermal system, Andean Cordillera, Northern Chile. *Clay Minerals*, 1-50.

Modelling Uncertainty and Data Group UoA. (2021). ccandu: conditional composition and uncertainty.

Orduz, J. (2019, March 23). *Sampling from a Multivariate Normal Distribution*. Retrieved from https://juanitorduz.github.io/multivariate_normal/

Renaud, T., Popineau, J., Riffault, J., O'Sullivan, J., Gravatt, M., Yeh, A., . . . O'Sullivan, M. (2021). Practical workflow for training in geothermal reservoir modelling. *Proceedings 43rd New Zealand Geothermal Workshop.* Wellington, New Zealand.

Zarrouk, S. J., & Simiyu, F. (2013). A review of geothermal resource estimation methodology. *35th New Zealand Geothermal Workshop.* Rotorua, New Zealand.